NJC

Accepted Manuscript

This article can be cited before page numbers have been issued, to do this please use: M. Teotia, N. Tarannum, M. Chauhan and R. K. Soni, *New J. Chem.*, 2019, DOI: 10.1039/C9NJ01560D.

This is an Accepted Manuscript, which has been through the Royal Society of Chemistry peer review process and has been accepted for publication.

Accepted Manuscripts are published online shortly after acceptance, before technical editing, formatting and proof reading. Using this free service, authors can make their results available to the community, in citable form, before we publish the edited article. We will replace this Accepted Manuscript with the edited and formatted Advance Article as soon as it is available.

You can find more information about Accepted Manuscripts in the author guidelines.

Please note that technical editing may introduce minor changes to the text and/or graphics, which may alter content. The journal's standard Terms & Conditions and the ethical guidelines, outlined in our author and reviewer resource centre, still apply. In no event shall the Royal Society of Chemistry be held responsible for any errors or omissions in this Accepted Manuscript or any consequences arising from the use of any information it contains.

ROYAL SOCIETY OF CHEMISTRY

rsc.li/njc

View Article Online
DOI: 10.1039/C9NJ01560D

Structure-based rational design, synthesis, crystal structure, DFT and molecular docking of 1,4 benzene dicarboxamide isomers with application as hardeners

MeenuTeotia[a], NaziaTarannum[a], MohitChauhan[a], and Rakesh Kumar Soni[a]
[a]Department of Chemistry, ChaudharyCharan Singh University, Meerut 250004, India
E-mail: teotiameenu@gmail.com, orcid.org/0000-0001-9833-7821, Phone: 09758154719

Abstract: N, N' di n-propyl (nPA) and N, N' diiso-propyl 1,4 benzene dicarboxamides (iPA), the two structural isomers have been successfully synthesized through aminolysis of poly(ethylene) terephthalate (PET) waste under catalyst free and ambient conditions. The compounds were characterized by elemental analysis, UV-visible spectroscopy, FTIR, ^{1}H- NMR and ^{13}C-NMR, mass spectrometry, Raman spectroscopy and SEM/EDX analysis. Single crystals of the isomers were grown in dimethylsulfoxide (DMSO) and analyzed through single crystal XRD to insight the crystal structure of the compounds (bond lengths and bond angles). Ab-initio Density Functional Theory (DFT) study has been executed at B3LYP (Becke's three parameter functional and Lee–Yang–Parr functional) using 6-31G basis set to investigate the physical parameters and theoretical calculation of crystal structures. The vibrational frequencies were optimized by DFT and found in close agreement with the experimental vibrational frequencies. The isomers crystallize in triclinic systems and the bond lengths and bond angles obtained with DFT calculations were in agreement with single crystal experimental data. The thermal characteristics of the derivatives was studied through TGA/DTA and DSC. Antimicrobial activity of the two isomers was assessed through molecular docking study with target proteins sterol 14 α-demethylase and Glucosamine-6-phosphate synthase. In order to validate isomers as hardeners for epoxy system, curing kinetic parameters were determined using isothermal method on DSC823^{e} kinetic software.

Keywords: aminolysis; depolymerization; SXRD; DFT; vibrational frequency; docking

View Article Online
DOI: 10.1039/C9NJ01560D

1. Introduction

Recycling of wastes has always been a global concern in order to minimize the harmful effects caused by disposal of wastes[1]. The concerned authorities face waste disposal problem and seekmethods to combat the adverse effects caused by accumulation of these wastes. PET is a well-known polymer used in the packaging of food, beverages and other liquid containers and occupies a large section in the piechart of plastic wastes. Due to large consumption of PET packed items, the amount of generated waste is very high demanding efficient recycling methods involving simpler and environmentally safer processes. Considerable research has been conducted towards chemical recycling of PET waste to obtain a number of useful products. Different techniques such as alcoholysis[2-4], aminolysis[5-7], ammonolysis[8-9], glycolysis[10-14], and hydrolysis[15-18] are being reported for depolymerization of PET. The whereabouts of these methods are available in ref Sinha et al., 2010[19]. Depolymerization of PET waste through aminolysis method gives aromatic amides which are least explored among the class of depolymerized end products obtained through chemical recycling techniques[20]. Most of the reported methods involves the use of catalysts and high temperature conditions. Metal chlorides[21], sulphates[22], acetates[22, 23-24], quaternary ammonium salts[6], imidazonium ionic liquids[25] etc. increase the electrophilicity of the carbonyl carbon of the PET backbone, hence facilitating the attack by amine nucleophile. However, the use of catalyst under high temperature conditions lead to harmful effects to the environment and the exposed manpower and also enhance the cost of commercialization of the developed technology. Microwave assisted techniques are also reported for depolymerization of PET[24, 26].

The use of terephthalamides in synthesis of polyurethanes[27], thiazolidine derivatives[28] has been revealed in literature. In previous works, terephthalic dihydrazide, an aminolysis product obtained through depolymerization of PET waste using hydrazine hydrate has been explored as plasticizer[29],

View Article Online
DOI: 10.1039/C9NJ01560D

antimicrobial agent[30] and also as a precursor to obtain UV curable acrylate oligomer[31]. However NN' dialkyl substituted terephthalamides are not that much reactive to be used in further acrylation reactions.

A lot of research is devoted to development of epoxy hardening systems as the later finds profound application in high performance fiber reinforced composites used in pressure moulding, filament winding and aerospace applications. The modified epoxy composites are also being used as transparent infills in manufacturing of laminated glasses which are extensively being used in structural and architectural applications[32-34]. Their application area is very wide which makes the knowledge of cure kinetics of the hardening systems an essential requisite to obtain controlled degree of cure[35-37].Generally compounds bearing amine functionalities are explored as curing agents for LY 556 resin[38]. Few reports reveal the use of polyamides as hardeners for epoxy resins[39-40]. The curing kinetics of a particular resin is of prime importance in order to optimize the curing temperatures as these reactions are initiated thermally but are exothermic. In this context, determination of energy of activation, rate constant, curing temperatures helps the end users for quality maintenance of the polymerized matrix[41-42].

In previous work, the authors successfully depolymerized PET waste through aminolysis method using methylamine, ethylene diamine, ethanolamine and butylamine at ambient conditions of temperature and pressure without using expensive and toxic catalysts to obtain respective 1,4 benzene dicarboxamides[43]. In the same series, two isomers, N,N' di n-propyl benzene 1,4dicarboxamide (nPA) and N, N' diiso-propyl benzene 1,4 dicarboxamide (iPA) have been obtained without using any catalyst at ambient temperature and pressure condition. The two compounds are structural isomers and characterized using FTIR, Raman spectroscopy, UV-visible spectroscopy, NMR (^{1}H and ^{13}C), mass spectrometry, elemental analysis and SEM/EDX analysis.

View Article Online
DOI: 10.1039/C9NJ01560D

The thermal characteristics of the compounds are investigated with the help of DSC and TGA. Single crystal study of the two isomers provided bond angles, bond lengths, crystal system and lattice parameters. DFT calculations have been performed to corroborate the vibrational frequencies and bond lengths and bond angles of the single crystals of the two isomers. The molecular docking study was performed for the compounds nPA and iPA with target protein sterol 14 α-demethylase and glucosamine-6-phosphate synthase to assess the antimicrobial activity. Herein, an attempt has also been made to inspect N, N' dialkyl substituted terephthalamides (synthesized structural isomers) as curing agents for LY 556 resin and curing kinetics is performed using isothermal method on DSC823^e software.

2. Material and Methods

2.1 Materials

Post consumed PET water bottles were collected and chopped into small flakes (4x4 mm) after removing cap. The flakes were washed with soapy water to remove dirt and other impurities and then with distilled water. The cleaned flakes were kept at 80 ^{0}C for 5 h and used for aminolysis reaction. N-propyl amine (99%), iso-propyl amine (99%), acetic acid (99.8%), acetone (99%), acetonitrile (99.8%),benzene (98%), chloroform (99.5%),dioxane (99.4%), dimethyl formamide (DMF; 99%), DMSO (99%), ethanol (99.9%),isopropyl alcohol (99%), toluene (99%), tetrahydrofuran (THF; 99.8%) and sodium hydroxide (97%) were procured from Fischer Scientific and used as received without further purification. Cyclohexane (99%) anddichloromethane (99%) were purchased from Merck and methanol (99%), n-heptane (99%),n-hexane (95%), triethanolamine (97%)were procured from Qualigen and used without any further treatment. Epoxy LY556 (density 1.15 g/cm^3), with epoxy index 5.30-5.45 eq/Kg and epoxy equivalent (ISO 3001) of 183-189 g/eq was procured from Huntsman.

View Article Online
DOI: 10.1039/C9NJ01560D

2.2 Characterization methods

Agilent FTIR Spectrometer (ATR module of Cary 630 FTIR, Agilent Technologies) was used to record FTIR spectra of the isomerswithin the range 600-4000 cm^{-1}. ^{1}H-NMR spectra were recorded on Multinuclear NMR spectrometer (9.4 T; 400 MHz) using DMSO solvent. ^{13}C-NMR spectra were obtained with FT NMR Spectrometer model Avance-II [Bruker at field strength 9.4 T (^{13}C frequency-100 MHz)] using DMSO solvent. UV spectra of the isomers were recorded on UV double beam spectrophotometer Systronics 2201, with band width 2 nm in DMSO solvent from 200-800 nm. Waters, Q-TOF Microma SS (LCMS) mass spectrometer was used to record mass spectra. Thermogravimetric (TG) and their derivative (DTG) curves were recorded on Perkin Elmer, Diamond TG/DTA at 20.00 ^{0}C/min in nitrogen atmosphere. Differential Scanning Calorimetric (DSC) curves of the isomers were recorded on DSC 7020 Hitachi Japan at heating rate of 10.00 ^{0}C/min in nitrogen atmosphere from 30 to 350 ^{0}C. Raman spectra were recorded on indigenously designed Raman spectrometer (RI Instruments & Innovation India). Elemental analysis was carried on Thermo Scientific (FLASH 2000) CHN Elemental Analyser.

SEM photomicrographs with different magnifications were obtained with Scanning Electron Microscope, ZIESS EVO 18. Energy dispersive X ray (EDX) experiments for percentage analysis of different elements was performed on EDAX AMETEK octane Pro-5301 operated at 70 kev. Concentrated solutions of the isomers in DMSO solvent were used to grow crystals in a vacuum sealed glass tube (8 mm o.d.). Single-crystal X-ray of the crystals for structural investigations was performed on a CCD Bruker SMART APEX diffractometer equipped with an Oxford Instruments low-temperature attachment. Graphite monochromated MoKa radiation with wavelength 0.71073 Å was used to collect data at temperature of 296(2) K. SMART and SAINT software packages were used to index, integrate and scale the frames[44], and SADABS program was used to correct

View Article Online
DOI: 10.1039/C9NJ01560D

the data for absorption[45]. The structures were solved and refined through SHELXL-2014/7 suite of programs[46]. Diamond 3.1e software has been used to generate crystallographic figures of nPA and iPA[47]. Crystal data of nPA and iPA has been deposited via joint CCDC/FIZ Karlsruhe deposition service and assigned the deposition numbers as 1903353 and 1903354 respectively.

2.3 Computational method

2.3.1. DFT Study

The quantum calculations were done using GAUSSIAN 03 program package[48]. DFT calculations were executed using Becke's three-parameter functional Lee-Yang-Parr functional (B3LYP) and 6-31G basis set was used for ground state geometry optimization[49-51].

2.3.2. Molecular Docking study

The molecular docking study was performed for the compounds nPA and iPA with target protein sterol 14 α-demethylase and glucosamine-6-phosphate synthase. D-fructose-6-phosphate amidotransferase (EC2.6.1.16) is also named as glucosamine-6-phosphate synthase (GlcN-6-P synthase)[52]. This enzyme undergoes hexosamine metabolism converting D-fructose 6-phosphate (Fru-6-P) into GlcN6P in the presence of glutamine as an ammonia source and finally forming an N-acetylglucosamine (NAG)[53]. NAG is used in cell wall formation in bacteria and fungi, such as peptidoglycan in bacteria and chitin, mannoproteins in fungi[54]. Sterol 14 α -demethylase (CYP51) belongs to cytochrome P450 superfamily and essential for fungal viability[55]. The enzyme is an important target to design antifungal agent as it catalyzes a key step in ergosterol biosynthesis in fungi in which methyl group is removed from the C-14 position in the sterol molecule[56-57]. The docking has been performed first using the default setting of standard precision (SP). Best pose has been selected on the basis of minimum binding energy and interactions with the respective protein space. Auto dock 4.2 was used for molecular docking[58]. Lamarkian genetic algorithm was used for molecular docking

View Article Online
DOI: 10.1039/C9NJ01560D

with population size of 150 and 0.8 cross over rate. Pymol was used for the visualization of interaction between protein-ligand complex[59]. The docked pose was then inspected by exploring the interactions between the receptor and ligands.

2.3.2.1. Ligand preparation: Chemical structure of nPA and iPA ligands were drawn with chemsketchtool[60]. The drawn structures were optimized with prodrg server[61].

2.3.2.2. Protein preparation: The 3D structures of proteins viz. (1). Sterol 14-alpha demethylase (CYP51B) from a pathogenic filamentous fungus *Aspergillusfumigatus* (PDB ID: 4UYM) and (2). Glucosamine-6-phosphate synthase (G6PS) from *Escherichia coli* (PDB ID: 1JXA) have been downloaded from RCSB PDB database (*https://www.rcsb.org/*). Protein pdb files were prepared for Molecular Docking. For protein preparation, heteroatoms and water molecules were deleted from pdb file.

2.4. Synthesis of N, N' di n-propyl and N, N' diiso-propyl 1,4 benzene dicarboxamides

Two structural isomers namely, N, N' di n-propyl 1,4 benzene dicarboxamide (nPA) and N, N' di iso-propyl 1,4 benzene dicarboxamide (iPA) were synthesized via aminolysis of PET waste through an environment friendly facile approach. The reactions were carried out in absence of catalysts under ambient conditions of temperature and pressure. 100 mL of n-propyl amine (Bottle A) and 100 mL of isopropyl amine (Bottle B) each were taken in separate sealed reagent bottles. 10 g of PET flakes were added to each bottle and the reagent bottle were sealed properly ensuring any escape of amine. The reaction products were collected after 25 and 48 days respectively. DMSO solvent was used to recrystallize the isomers and freshly recrystallized compounds were subjected to FTIR, ^{1}H-NMR, ^{13} C-NMR, UV-visible, mass spectrometry, S-XRD, thermal, Raman and elemental analysis. The respective theoretical and experimental percentages of carbon,

View Article Online
DOI: 10.1039/C9NJ01560D

hydrogen, nitrogen and oxygen of the two structural isomers with the molecular formula $C_{14}H_{20}N_2O_2$ are shown as:

nPA, C= (67.74%) (68.01%); H= (8.06%) (8.12%); N= (11.29%) (11.08%),

iPA, C= (67.74%) (68.24%); H= (8.06%) (8.23%); N= (11.29%) (11.01%).

2.5. Curing kinetic studies

Formulations comprising epoxy resin and structural isomers were prepared in 1:1 mole ratio and dynamic thermal curves were obtained. No curing peaks were observed for these formulations as the hydrogen bonded to nitrogen is secondary and the lone pair of nitrogen is involved in resonance with carbonyl group. Hence, sodium hydroxide (2%) and triethanolamine (1%) were used as catalyst and initiator respectively. Samples were weighed in aluminium pans and dynamic curve for each formulation were recorded from 30 to 350 ^{0}C at heating rate of 10 ^{0}C/minute on Differential scanning calorimeter using modulated DSC. On the basis of curing peak temperatures, certain temperatures (100, 105 and 110 ^{0}C) were chosen for curing kinetic studies through isothermal method using DSC823^{e}star kineticsoftware. Three isothermal runs were recorded for each formulation. Energy of activation (Ea), rate constant (In K) and order of reaction (n) were estimated and compared with the help of isothermal curves kinetic analysis. The basic equation for nth order kinetics is:

$$\frac{d\alpha}{dt} = K(1-\alpha)^n \qquad \text{Equation 1}$$

The values of $\frac{d\alpha}{dt}$ and α were used to calculate K and n for actual temperatures. With three isothermal measurements, the kinetic data, In K and E_A were calculated and for n, mean value of the individual results was used.

View Article Online
DOI: 10.1039/C9NJ01560D

The vibrational frequencies of formulations FnPA and FiPA and cured filmswere obtained after dynamic runsfrom 600-4000 cm^{-1} in order to ensure the participation of amides in the crosslinked network.

3. Results and Discussion

The two structural isomers were obtained through depolymerisation of PET via aminolysis reaction with n-propylamine and isopropylamine at ambient conditions of temperature and pressure. Bottle A, with nPA showed needle like crystals within two days and only partial swelling of PET flakes was observed for iPA (Bottle B) even after 4 days. N-propylamine depolymerised PET flakes completely in 25 days, however nearly 50% conversion was achieved for isopropylamine (Bottle B). The nucleophilic nitrogen of isopropylamine is attached to an isopropyl group which results in a sterically hindered approach of the nucleophile to attack the carbonyl carbon of PET backbone, therefore more time was required in generation of precipitate. Rate of degradation was also slower and aminolytic degradation of all the folds of PET with isopropylamine was completed in 48 days. The synthesis was carried out in absence of catalyst and high temperature eliminating the disadvantage associated with catalytic depolymerization at high temperature[43].

3.1 Solubility

Table 1 depicts the typical solubilities of isomers nPA and iPA in different solvents. The isomers were dissolved in excess of solvents at 30 ± 2 ^{0}C, stirred and kept for 10 h. They dissolved completely in DMSO, DMF, THF and acetic acid. nPA is soluble in ethyl alcohol and isopropyl alcohol, however, iPA is completely soluble in the mentioned solvents after heating.

View Article Online
DOI: 10.1039/C9NJ01560D

3.2 FTIR Analysis

FTIR spectra of the isomers were recorded on Attenuated Total Reflection module in solid state, as shown in Figure 1. The experimental and theoretical (calculated through DFT) vibrational frequencies (cm^{-1}) corresponding to important functional groups have been compared in Table 2. The two prominent absorptions in the region 3294.274 and 3303.427 $cm^{-1}$and 1622.48 and 1625.35 cm^{-1} are attributed to N-H stretch and C=O stretch, (characteristic bands of amides for compounds nPA and iPA). The complete aminolysis of PET flakes was achieved as indicated from the absence of peak near 1715 cm^{-1}, corresponding to C=O stretch of ester linkage in both the spectra. The vibrational frequencies of the isomers were further confirmed by complementary characterization technique Raman spectroscopy. Raman spectra of the isomers have been provided in the supplementary files (Figure S1).

Table 1: Solubility of isomers (nPA&iPA) in different solvents[1]

Solvent	nPA	iPA
Acetic acid	+	+
Acetone	--	--
Acetonitrile	--	--
Benzene	--	--
Chloroform	--	--
Cyclohexane	--	--
Dichloromethane	+*	+*
Dioxane	+*	+*
Distilled water	--	--
DMF	+	+
DMSO	+	+
Ethanol	+	+*
Isopropyl Alcohol	+	+*
Methanol	--	--
n-heptane	--	--
n-hexane	--	--
THF	+	+
Toluene	--	--

[1]**[(+) =soluble (--) =insoluble (+*) = solubility on heating]**

View Article Online
DOI: 10.1039/C9NJ01560D

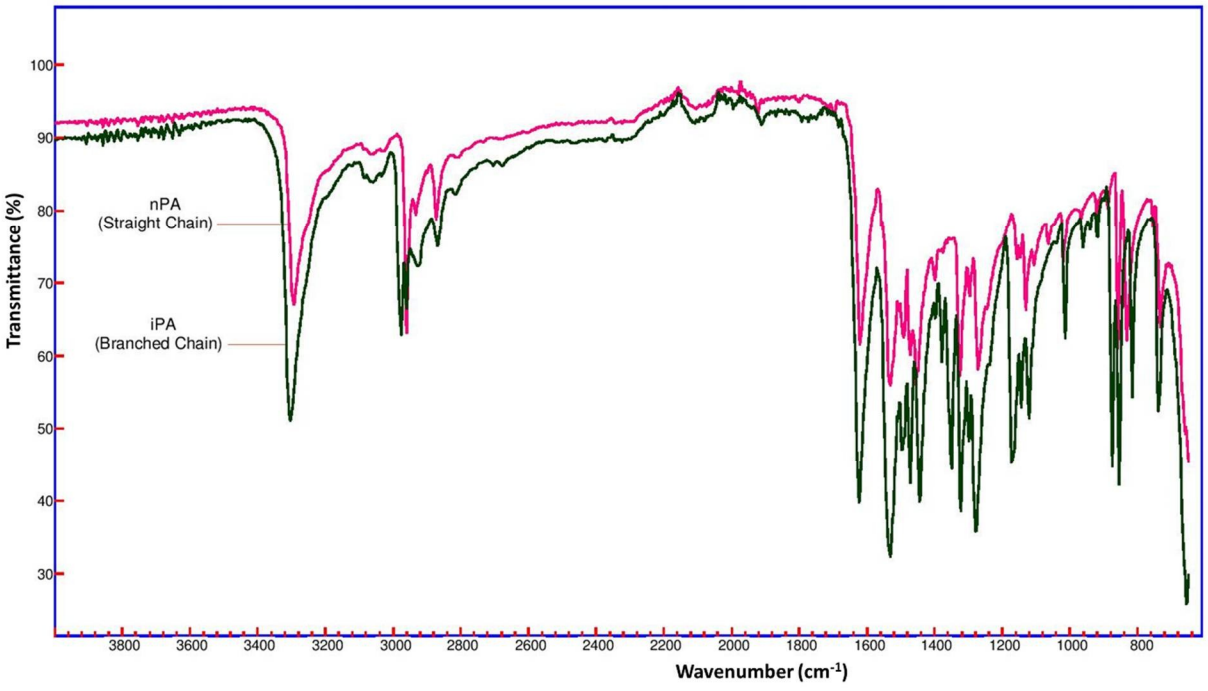

Figure 1: FTIR spectra of nPA (N, N' di n-propyl) and iPA (N, N' di-isopropyl) 1,4 benzene dicarboxamides

Table 2: Experimental and theoretical vibrational frequencies of nPA and iPA with respect to functional groups

Amides/ Type of Vibration	**nPA**		**iPA**	
	Experimental	DFT Study	Experimental	DFT Study
N-H Stretch	3294	3296	3303	3300
C=O stretch (Amide I band)	1622	1621	1625	1631
C=C stretch	1534	1530	1534	1530
	1496	1496	1496	1498
	1455	1440	1446	1443
C-N Stretch	1133	1137	1123	1126
			1174	1167

View Article Online
DOI: 10.1039/C9NJ01560D

3.3 NMR Characterization

^{1}H-NMR spectra of compounds nPA and iPA are shown in Figure 2. ^{1}H-NMR spectrum for nPA shows typical resonances: a triplet at 0.9 δ (3H) due to methyl protons; a multiplet at 1.5 δ (2H) is attributed to –CH_2 protons directly bonded to methyl carbon; a multiplet at 3.2 δ (2H) for –CH_2 protons directly bonded to nitrogen atom of amide group; a very strong peak at 7.8 δ (4H) due to aromatic protons and a triplet at 8.6 δ (1H) attributed to –NH protons. The peaks obtained in ^{1}H-NMR spectrum for iPA are attributed as: a doublet at 1.19 δ (6H) for methyl protons; a multiplet at 4.1 δ (1H) due to –CH protons; a sharp singlet at 7.9 δ (4H) for aromatic protons and a doublet at 8.4 δ (1H) due to –NH protons. A very strong absorption at 3.3 δ is due to the presence of residual water in DMSO and a peak at 2.5 δ is attributed to residual d_5 DMSO in both the spectra[62-63].

Figure 3 depicts ^{13}C-NMR of nPA and iPA in DMSO solvent.^{13}C NMR of nPA shows peaks at: 11.23 δ (2C, a); 22.27 δ (2C, b); 40.24 (2C, c); 165.99 δ (2C, d); 136.71 δ (2C, e) and 126.79 δ (4C, f). The typical ^{13}C NMR resonances of iPA are attributed at, 22.08 δ (4C, a); 40.22 δ (2C, b); 165.38 δ (2C, c); 136.81 δ (2C, d) and 126.74 δ (4C, e). Peaks present at 39.75 δ and 78.96 δ are due to methyl carbons of DMSO and $CHCl_3$ respectively[62-63]. Hence, the two structural isomers show nearly similar absorptions except for the side chain carbons.

View Article Online
DOI: 10.1039/C9NJ01560D

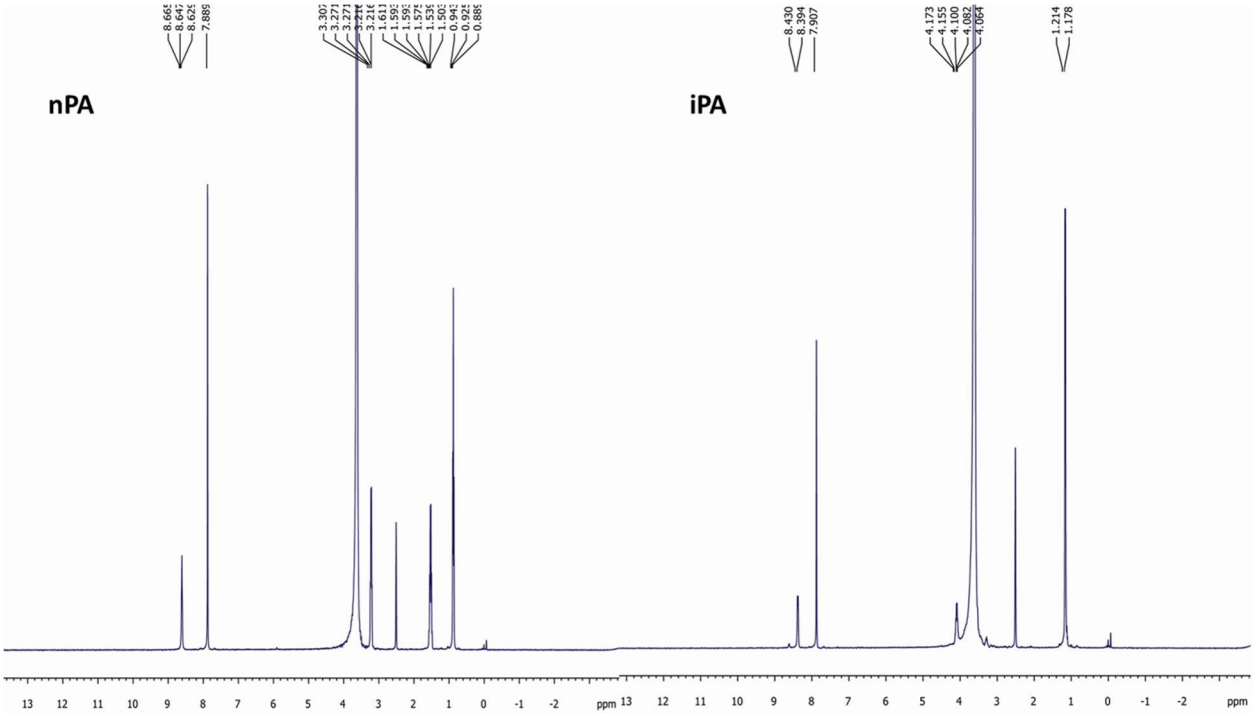

Figure 2: ^{1}H NMR spectra of nPA (N, N' di n-propyl) and iPA (N, N' di-isopropyl) 1,4 benzene dicarboxamides

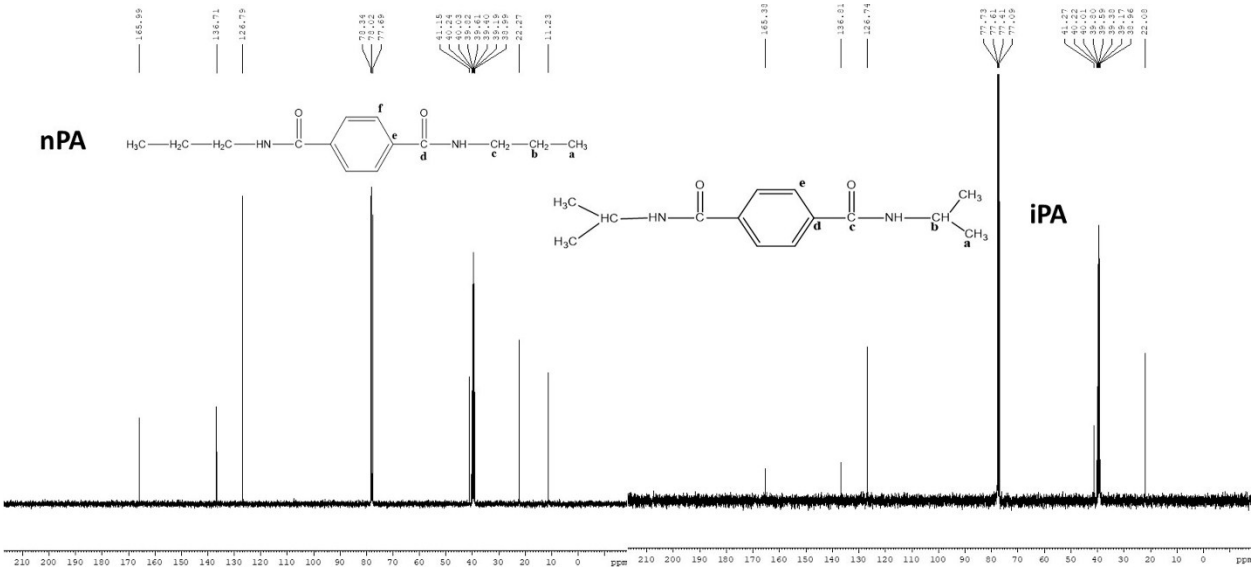

Figure 3: ^{13}C NMR spectra of nPA (N, N' di n-propyl) and iPA (N, N' di-isopropyl) 1,4 benzene dicarboxamides

View Article Online
DOI: 10.1039/C9NJ01560D

3.4 UV-visible Absorption

Solutions of nPA and iPA were prepared in DMSO (1mg/10 mL) and irradiated with UV-visible radiations in 1 cm path quartz cells. UV-visible spectra obtained were quite similar for both the isomers as the chromophore is same showing very strong absorption in the range 250-300 nm with λ_{max}value at 268 nm (Figure S2). The molecules undergo π-π* transition due to -HNCO-C_6H_4-CONH- group and showed two absorption bands, one intense band at 268 nm and another one at 292 nm.

3.5 Mass Spectral Analysis

Mass spectra of nPA and iPA were recorded using electrospray ionization technique (Figure S3). The high resolution MS spectra show molecular ion peaks [M] ionized by H^+, peaks at m/z corresponding to their metal adducts and also their dimers[64]. The molecular masses of both compounds were observed as 248.14 from their $[M+H]^+$ peaks. The mass spectrum of nPA shows base peak at m/z 249.14 (100%) which corresponds to $[M+H]^+$; peak at m/z 250.16 (38%) for $[M+2H]^+$; peak at m/z 271.16 (18%) for $[M+Na]^+$; peak at m/z 497.36 (9%) for dimer $[2M+H]^+$; peak at m/z 519.34 (8%) for dimer $[2M+Na]^+$ and a peak at m/z 565.34 (7%) for dimer $[2M+Na]^+$. In the same way, mass spectrum of iPA reveals base peak at m/z 249.15 (100%) which corresponds to $[M+H]^+$; peak at m/z 250.17 (38%) for $[M+2H]^+$; peak at m/z 271.16 (22%) for $[M+Na]^+$; peak at m/z 497.36 (5%) for dimer $[2M+H]^+$; peak at m/z 519.34 (7%) for dimer $[2M+Na]^+$ and a peak at m/z 565.34 (3%) for dimer $[2M+Na]^+$. A peak at m/z 207.13 (8%) in the mass spectrum of iPA is attributed to fragment of molecular ion after loss of isopropyl group i.e., $[M+2H-CH(CH_3)_2]^+$, which is absent in mass spectrum of nPA.

View Article Online
DOI: 10.1039/C9NJ01560D

3.6 Thermal Characterization

The crystallized aminolysed end products were subjected to TGA and DSC analysis of depolymerized aminolysates in order to investigate their physical characteristics and decomposition behaviour at high temperatures. Although, the two compounds are isomers with difference of branched and unbranched propyl chain attached to nitrogen atom, which is contributing to a difference in their melting points, enthalpy change and their decomposition temperature.The compound nPA follows single step degradation with maximum weight loss (92%) between 295-370^{0}C with peak maxima at 355.97 ^{0}C at a rate of 1.452 mg/min leaving 8% char (Figure 4). The melting point of compound nPA was found as 241.60 ^{0}C from DSC curve (Figure 5) with 48.6 J/g enthalpy of melting. The DSC peak is followed by broad exothermic hump which may be referred to recrystallization of compound nPA.

The decomposition profile of iPA involves two steps with peak maxima at 339.33 ^{0}C and 445.07 ^{0}C corresponding to ~48% and 35% weight loss, respectively (Figure 4). The first step can be attributed to loss of two propene and two ammonia molecules which correspond to 47.58% weight of the compound. The expulsion of neutral molecule propene is further confirmed by the presence of peak at 207 m/z in its mass spectrum (Figure S2). The second peak in DTG curve may correspond to evolution of carbon monoxide and carbon dioxide leaving nearly 9% char residue. Freshly recrystallized and dried sample of compound iPA was used for DSC and scans were collected in triplicate. DSC thermogram of compound iPA depicts a very sharp peak at 284 ^{0}C clearly indicating its melting point with 106 J/g enthalpy of melting, which is very high in comparison to nPA suggesting highly crystalline nature of the compound. A small endothermic peak is also seen at 268 ^{0}C. Generally, polymorphic crystalline compounds exhibit such peaks for

View Article Online
DOI: 10.1039/C9NJ01560D

metastable forms which then convert to stable forms. The study suggested iPA to be polymorphic crystalline solid.

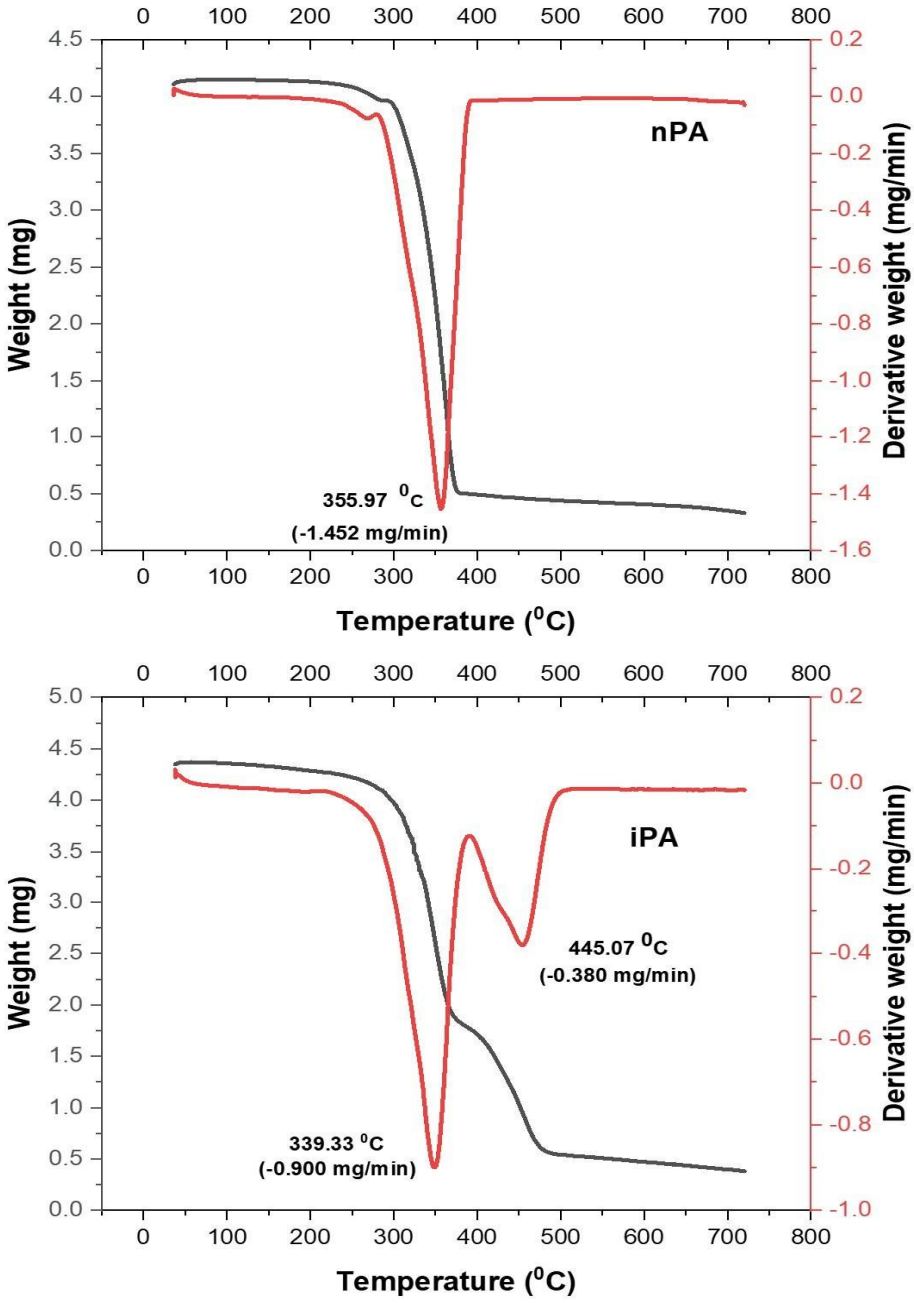

Figure 4: TGA/DTG curves of nPA (N, N' di n-propyl) and iPA (N, N' di-isopropyl) 1,4 benzene dicarboxamides

View Article Online
DOI: 10.1039/C9NJ01560D

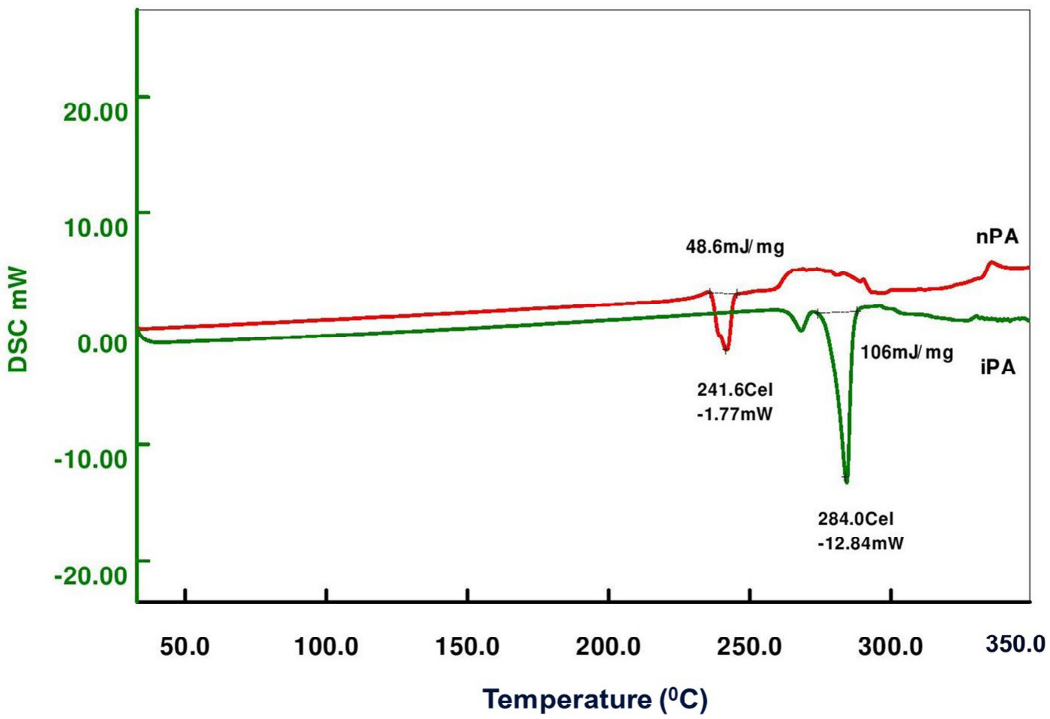

Figure 5: DSC curves of nPA (N, N' di n-propyl) and iPA (N, N' di-isopropyl) 1, 4 benzene dicarboxamides

3.7 SEM Analysis

SEM photomicrographs of compound nPA and iPA with 500 X magnification (Figure 6) depict crystalline nature of both isomers. Long needle like crystals are seen which have been identified as triclinic crystal system through S-XRD studies. The carbon weight percentage obtained through EDX experiments for compounds nPA and iPA are 67.96% and 66.75% respectively which were in accord with elemental analysis of the two structural isomers.

View Article Online
DOI: 10.1039/C9NJ01560D

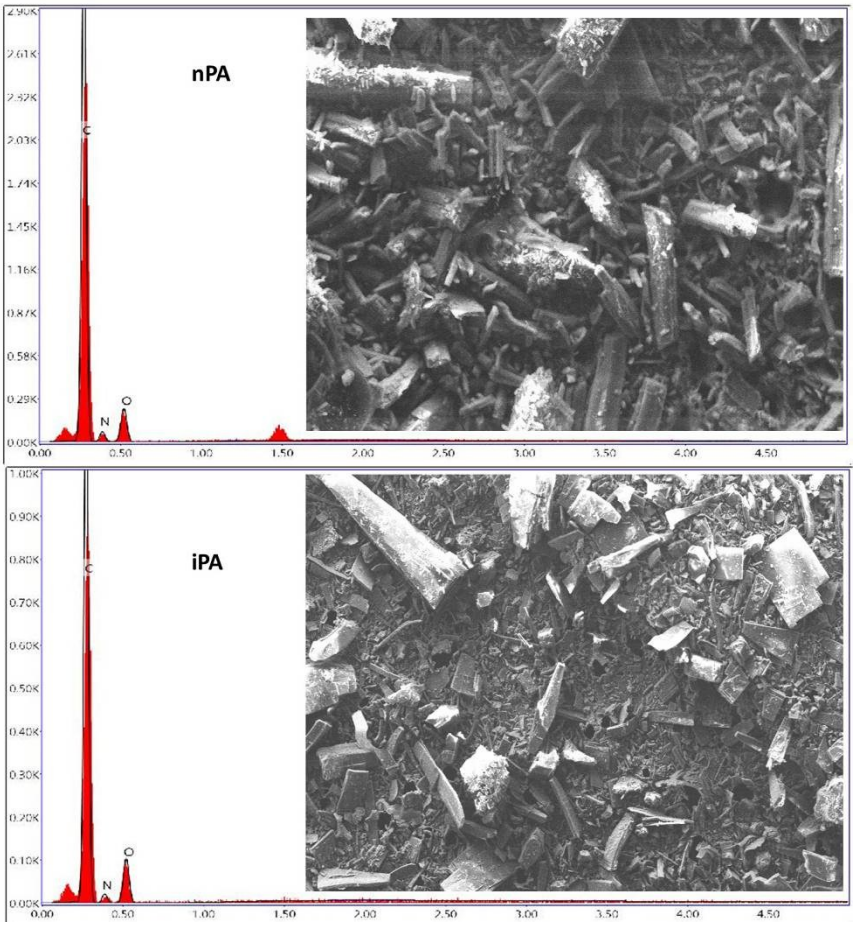

Figure 6: SEM photomicrographs with 500 X magnification/EDX analysis of nPA (N, N' di n-propyl) and iPA (N, N' di-isopropyl) 1, 4 benzene dicarboxamides

3.8 Single crystal (S-XRD) studies

Freshly recrystallized samples were used for S-XRD to collect crystal data and structure refinement. The identified crystal system is triclinic for both isomers which is least symmetric among crystal systems, centrosymmetric with pinacoidal class and with space group $P\bar{1}$. The unit cell dimensions observed for crystal nPA and iPA are depicted in Table 3. The calculated bond lengths and bond angles are listed in Table 4 and 5. The three bond angles for carbonyl carbon of compound nPA, C3C4N1, C3C4O1 and N1C4O1 are $117.4(2)^0$, $121.3(3)^0$ and $121.3(3)^0$ respectively. The distortion in values from trigonal planar geometry is due to repulsive interaction

View Article Online
DOI: 10.1039/C9NJ01560D

of lone pairs of oxygen atom with ortho hydrogen of benzene ring. The similar distortion was observed for compound iPA with slight increase in N1C4O1 angle (121.7^0) due to presence of two methyl groups on the carbon bonded to nitrogen atom. The crystallographic figures of the two structural isomers are shown in Figure 7.

Table 3: Unit cell dimensions of nPA and iPA crystals obtained through SXRD analysis[2]

	nPA	iPA
a (Å)	5.0286(19)	5.0619(16)
b (Å)	7.660(3)	5.1565(17)
c (Å)	9.751(4)	13.593(4)
α (Å)	105.952(9)°	100.634(8)°
β (Å)	95.479(9)°	96.239(8)°
γ (Å)	106.190(9)°	95.839(8)°
Volume ($Å^3$)	340.7(2)	343.93(19)

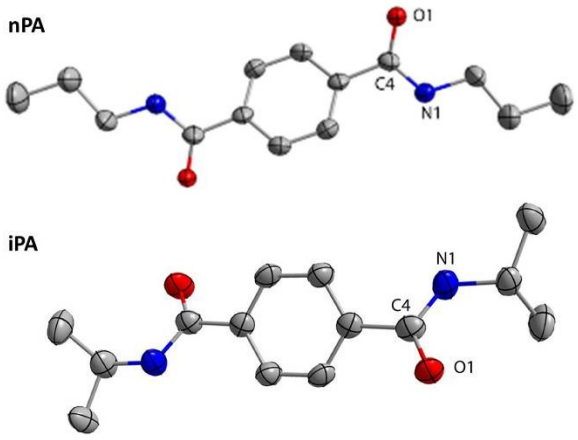

Figure 7: Crystallographic structures with important atoms labeled of compound nPA and compound iPA obtained through Diamond 3.1e software (Hydrogen atoms have been omitted for clear view of carbon skeleton)

[2]a, ≠ b, ≠ cand α, ≠ β,≠ γ

View Article Online
DOI: 10.1039/C9NJ01560D

3.9 Density Function Theory (DFT) Study:

The theoretical study of the isomers were performed at DFT/B3LYP 6-31G basis set method. Several parameters for the geometry of the isomers are calculated. Several calculated thermodynamic parameters have been presented in Table 6. The value of the dipole moment of nPA and iPA was found to be 6.2778 and 6.9593 Debye respectively. The electrostatic field is pulled in case of iPA as compared to nPA thereby increase the dipole moment value. Both the molecules have C1 symmetry showing low energy at all levels. Mulliken atomic charges of the two molecules have been presented as supplementary data (Table TS1). The total energy of the molecule is the sum of rotational, vibrational, electronic and translational energies. The experimental bond length and bond angles of the two compounds were compared with DFT data (Table 4 and 5). The theoretical and experimental vibrational frequencies of the two compounds were also compared and found to be in accordwith experimental data (Table 2). DFT also helped in comparing the bond lengths and bond angles of the two isomers with that of S-XRD data (Table 4 and 5).

Table 4: Comparative table for bond lengths [Å] of crystals of nPA and iPA crystals obtained through SXRD and DFT calculations

Bond lengths	nPA		Bond lengths	iPA	
	SXRD	DFT		SXRD	DFT
O1 C4	1.233	1.255	O1 C4	1.239	1.256
N1 C4	1.337	1.371	N1 C4	1.331	1.376
N1 C5	1.459	1.466	N1 C5	1.451	1.478
N1 H1A	0.8600	1.008	N1 H1A	0.8600	1.015
C3 C1	1.382	1.404	C2 C1	1.379	1.405
C3 C2	1.386	1.405	C2 C3	1.380	1.404

View Article Online
DOI: 10.1039/C9NJ01560D

C3 C4	1.488	1.498	C2 C4	1.492	1.498
C1 C2	1.382	1.392	C1 C3	1.370	1.392
C1 C3	1.382	1.405	C1 H1	0.9300	1.083
C1 H1	0.9300	1.085	C3 C1	1.370	1.397
C2 H2	0.9300	1.085	C3 H3	0.9300	1.083
C5 C6	1.488	1.543	C5 C6	1.496	1.538
C5 H5A	0.9700	1.093	C5 C7	1.507	1.540
C5 H5B	0.9700	1.099	C5 H5	0.9800	1.093
C6 C7	1.516	1.536	C6 H6A	0.9600	1.095
C6 H6A	0.9700	1.096	C6 H6B	0.9600	1.094
C6 H6B	0.9700	1.099	C6 H6C	0.9600	1.097
C7 H7A	0.9600	1.096	C7 H7A	0.9600.	1.095
C7 H7B	0.9600	1.095	C7 H7B	0.9600	1.097
C7 H7C	0.9600	1.097	C7 H7C	0.9600	1.096

Table 5: Comparative table for bond angles [°] of crystals of nPA and iPA crystals obtained through SXRD and DFT calculations

Bond Angle	nPA		Bond Angle	iPA	
	SXRD	DFT		SXRD	DFT
C4 N1 C5	121.3	121.7	C4 N1 C5	122.6	125.8
C4 N1 H1A	119.3	119.5	C4 N1 H1A	118.7	112.8
C5 N1 H1A	119.3	118.2	C5 N1 H1A	118.7	115.7
C1 C3 C2	118.4	119.0	C1 C2 C3	118.4	118.9

View Article Online
DOI: 10.1039/C9NJ01560D

C1 C3 C4	122.8	123.7	C1 C2 C4	118.8	117.8
C2 C3 C4	118.8	117.6	C3 C2 C4	122.8	122.9
O1 C4 N1	121.3	121.7	O1 C4 N1	121.7	120.3
O1 C4 C3	121.3	121.2	O1 C4 C2	121.0	120.0
N1 C4 C3	117.4	116.9	N1 C4 C2	117.3	119.6
C2 C1 C3	120.7	120.4	C3 C1 C2	120.8	120.5
C2 C1 H1	119.7	118.9	C3 C1 H1	119.6	120.7
C3 C1 H1	119.7	120.51	C2 C1 H1	119.6	118.6
C1 C2 C3	120.9	120.4	C1 C3 C2	120.8	120.5
C1 C2 H2	119.6	121.4	C1 C3 H3	119.6	121.1
C3 C2 H2	119.6	121.5	C2 C3 H3	119.6	118.2
N1 C5 C6	112.7	113.4	N1 C5 C6	110.6	110.5
N1 C5 H5A	109.1	106.9	N1 C5 C7	111.4	110.5
C6 C5 H5A	109.1	106.9	C6 C5 C7	111.2	111.6
N1 C5 H5B	109.1	108.2	N1 C5 H5	107.8	106.9
C6 C5 H5B	109.1	108.2	C6 C5 H5	107.8	109.2
H5A C5 H5B	107.8	108.1	C7 C5 H5	107.8	108.3
C5 C6 C7	112.1	111.9	C5 C6 H6A	109.5	110.6
C5 C6 H6A	109.2	108.3	C5 C6 H6B	109.5	111.4
C7 C6 H6A	109.2	110.1	H6A C6 H6B	109.5	108.5
C5 C6 H6B	109.2	109.3	C5 C6 H6C	109.5	110.6
C7 C6 H6B	109.2	110.1	H6A C6 H6C	109.5	107.8
H6A C6 H6B	107.9	106.9	H6B C6 H6C	109.5	107.8

View Article Online
DOI: 10.1039/C9NJ01560D

C6 C7 H7A	109.5	111.0	C5 C7 H7A	109.5	110.6
C6 C7 H7B	109.5	111.1	C5 C7 H7B	109.5	110.7
H7A C7 H7B	109.5	107.8	H7A C7 H7B	109.5	107.8
C6 C7 H7C	109.5	111.3	C5 C7 H7C	109.5	110.8
H7A C7 H7C	109.5	107.7	H7A C7 H7C	109.5	108.4
H7B C7 H7C	109.5	107.8	H7B C7 H7C	109.5	108.2

Table 6: Theoretically calculated physical and thermodynamic parameters of isomers nPA and iPA

Parameters	nPA	iPA
Dipole moment (Debye)	6.2778	6.9593
Total energy (Kcal/mol)	212.91	212.55
Total Cv (Cal/mol K)	52.71	55.34
Entropy (S) (Cal/mol K)	112.58	112.80
Zero point vibrational energy (Kcal/mol)	204.96	204.47
Thermal correction to Energy	0.3393	0.3387
Thermal correction to Enthalpy	0.3402	0.3396
Degree of freedom	108	111
Full point group	C1	C1
Thermal correction to Gibbs free energy	0.2867	0.2860

3.10 Molecular Docking

The molecular docking study was performed for the compounds nPA and iPA with target protein sterol 14 α-demethylase (4uym) and glucosamine -6-phosphate synthase (1jxa). The two isomers showed antimicrobial activity. The two ligands nPA and iPA were incorporated within 4uym in the same cavity and space. The binding site in the protein was found to have sufficient volume and area

View Article Online
DOI: 10.1039/C9NJ01560D

which can accommodate ligands in the cavity because of its shape and size. The interaction between the protein (4uym) and ligands are due to non-covalent interactions along with hydrogen bond (H-bond) to achieve proper binding. nPA is forming 1 H bond with the protein and the interacting amino acid are Lue304, Gly308, Phe468, Gly465, Ser311, Ser312, Ala469, Leu154, Phe456 which are labelled in the Figure 8. The amino acids of protein residues that interacted with iPA are Ser312, Ser311, Ala469, Leu387, Gly465, Phe456, Gly308, Gly465, Phe456. nPA showed better binding with the protein as compared to iPA. The antifungal activity can be predicted to be good in nPA as compared to iPA. Table 7 shows minimum binding energy of compounds with two target proteins.

Table 7: Minimum binding energy of docked compounds (nPA and iPA) in two different proteins: sterol 14 α-demethylase (4uym) and glucosamine -6-phosphate synthase (1jxa)

Ligands	Minimum Binding Energies with 4uym (Kcal/mol)	Hydrogen bonds formed between ligand and target protein	Interacting Amino Acids
nPA	-7.88	1	Lue304,Gly308,Phe468,Gly465,Ser311,Ser312 ,Ala469,Leu154,Phe456
iPA	-6.01		Ser312,Ser311,Ala469,Leu387,Gly465,Phe456 ,Gly308,Gly465,Phe456
Ligands	Minimum Binding Energies with 1jxa (Kcal/mol)	Hydrogen bonds	Interacting Amino Acids
nPA	-4.92	1	Lys603,ala602,val605,leu601,ser349,leu501,as n365,pro377,asn392
iPA	-5.06	1	Ser604,ser349,gln348,lys603,ser401,leu501,leu 601,ser349,leu484

The binding site of glucosamine-6-phosphate synthase (1jxa) is formed mainly by the loop which can be considered as highly flexible area and not having very deep pocket. Because of its shallow nature, cavity is exposed to water and abundantly by lipophilic residues in the region but also has

View Article Online
DOI: 10.1039/C9NJ01560D

some hydrophobic residue in the interior[65] (Figure 8 (b)). This is the reason why the two ligands appear to show moderate binding score with 1jxa. The interacting amino acids found for iPA are Ser604, ser349, gln348, lys603, ser401, leu501, leu601, ser349, leu484 and forms 1 H bond. In case of nPA, the interacting amino acids found are Lys603, ala602, val605, leu 601, ser349, leu501, a sn365, pro377, asn392 and forms 1 H bond. The minimum binding energy for iPA was greater than nPA. The results have shown that the ligands are more susceptible to antifungal activity as compared to antibacterial study.

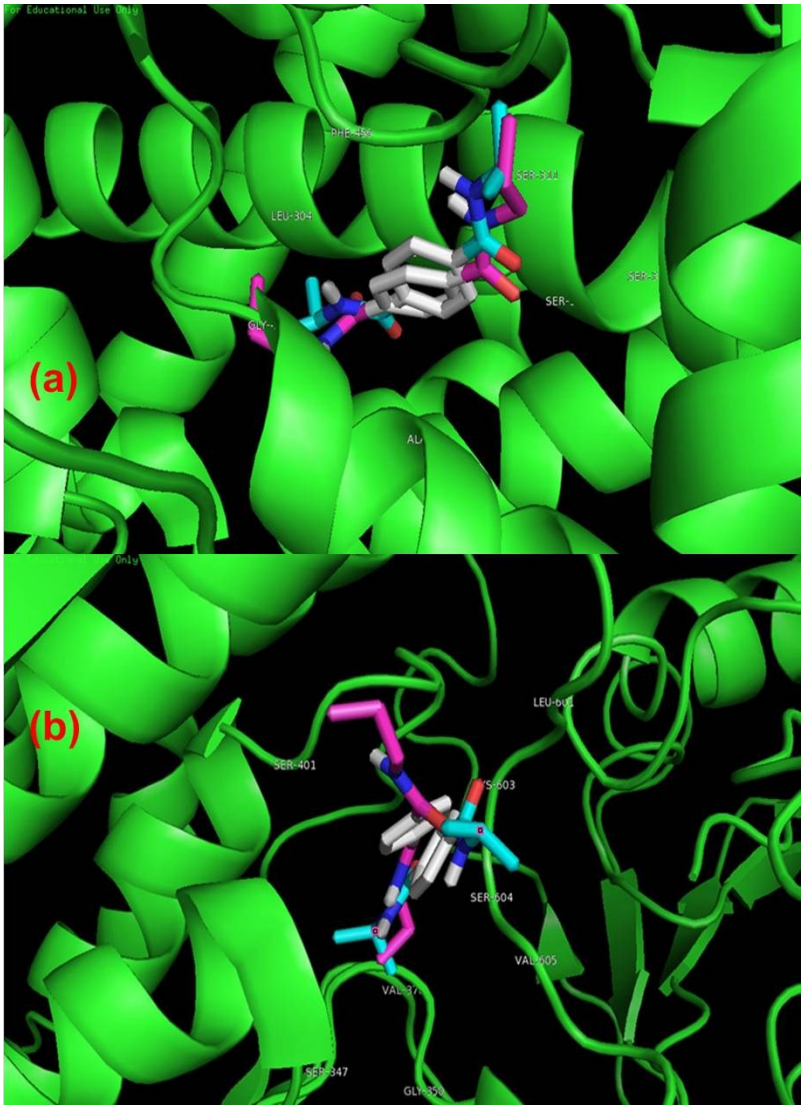

View Article Online
DOI: 10.1039/C9NJ01560D

Figure 8: (a) Docking pose of two ligands in the binding site of sterol 14-alpha demethylasefrom a pathogenic filamentous fungus *Aspergillusfumigatus* (PDB ID: 4UYM) and (b) docking pose of two ligands in the binding site of glucosamine-6-phosphate synthase from *Escherichia coli* (PDB ID: 1JXA)

3.11 Curing Kinetics

Dynamic curves of Fnpa and Fipa are depicted in Figure 9. Broad curing peaks were observed in temperature range 30-350 ^{O}C. The films obtained after DSC analysis were subjected to FTIR analysis to ensure epoxy ring opening and participation of 1,4 benzene dicarboxamides (Figure S4). Absence of N-H stretch bands in the FTIR spectra of cured samples confirm the participation of amides in the polymerized matrix. Sodium hydroxide helps in epoxy ring opening making the carbon to be attacked more electron deficient, hence pushing the reaction in forward direction. Three isothermal runs were conducted for each formulation shown in Figure 10 for FnPA (a) and FiPA (b), respectively. The curing kinetic data (Table 8) shows higher activation energy for FnPA formulation by 3.16 KJ/mol, however order of the reaction was found 0.57 and 0.58 for FnPA and FiPA, respectively. The conversion tables reveal slightly faster polymerization in FiPA and lower activation energy.

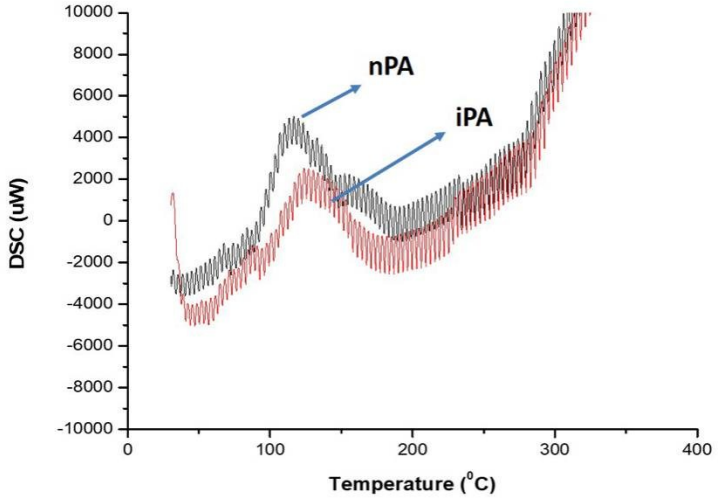

Figure 9: Dynamic curves of FnPA and FiPA formulations from 30-350 ^{0}C

View Article Online
DOI: 10.1039/C9NJ01560D

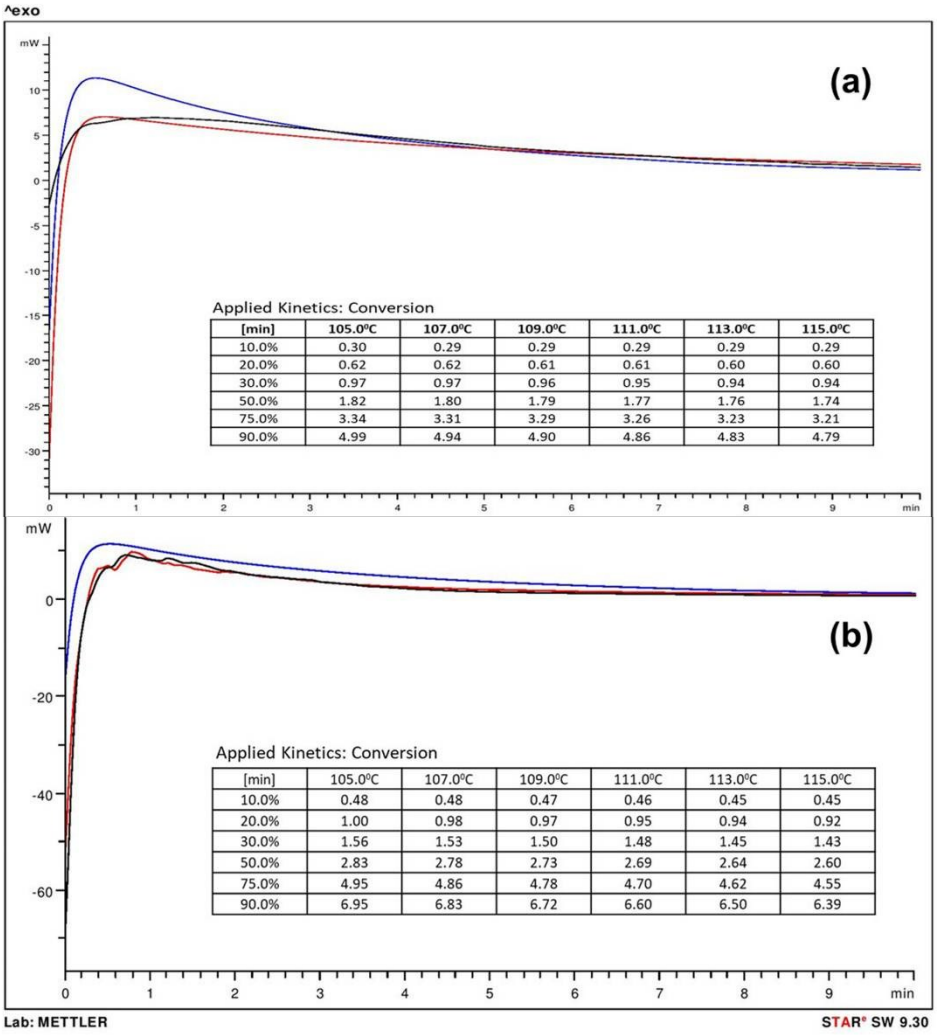

Figure 10: Isothermal curves of (a) FnPA and (b) FiPA formulation at 100, 105 and 110 ^{0}C

Table 8: Curing kinetic parameters obtained through isothermal method

S. No.	Kinetic parameters	FnPA	FiPA
1.	In(K_0)	-1.35	-2.36
2.	E_A KJ/mol	13.49	10.33
3.	n	0.57	0.58

View Article Online
DOI: 10.1039/C9NJ01560D

4. Conclusion

With effect to growing need for PET bottles as packaging material, it is extremely important to develop efficient chemical recycling method on their disposal. The current study deals with the synthesis and structural analysis of generated waste efficient aromatic carboxamides. The two structural isomers of 1,4 benzene dicarboxamide have been successfully synthesized through depolymerization of PET without using catalysts at room temperature conditions. The characterization data obtained confirms the structures as N, N' di n-propyl and N, N' di-isopropyl 1,4 Benzene dicarboxamides. The two isomers possess C1 point group and show triclinic crystalsystem. Bond angles and bond lengths were obtained through S-XRD technique and were found in good accord with DFT simulated values. An effort has been putforth to investigate the curing characteristics of two structural isomers to be used as epoxy hardeners for LY556 resin. The compounds were crosslinked in epoxy network in presence of catalyst and initiator and depicted close conversion characteristics. iPA was investigated as slightly faster curing agent owing to its positive inductive effect at nitrogen atom flanked by two methyl groups. The future work envisages the conversion of amides to amines to make them active curing agents eliminating the need of catalyst and initiators that may cause the depletion of finally cured networks over a time range. Further, molecular docking of the isomers were studied for target proteins sterol 14α-demethylase, and glucosamine-6-phosphate synthase. The binding energy and interaction between the target protein and ligand have been studied. The antifungal activity was found to be potentially good for nPA as compared to iPA.

Conflicts of interest: There are no conflicts to declare.

View Article Online
DOI: 10.1039/C9NJ01560D

Acknowledgement: Authors would acknowledge DST (DST/TSG/Ceramic/2011/77-G) for the financial assistance. Authors would also like to acknowledge SAIF Centre, Punjab University and Cochin for carrying out NMR, MS and TGA/DTA analysis.

References

1. A. Mittal, M. Teotia, R. K. Soni and J. Mittal, *J. Mole. Liq.*, 2016,223, 376-387. https://doi.org/10.1016/j.molliq.2016.08.065
2. M. Goto, H. Koyamoto, A. Kodama, T. Hirose and S. Nagaoka, *J. Phys. Condens. Matter.*, 2002, 14, 11427-11430.
3. Y. Yang, Y. Lu, H. Xiang, Y. Xu and Y. Li, *Polym. Degrad. Stab.*, 2002, 75, 185-91. https://doi.org/10.1016/S0141-3910(01)00217-8
4. M. Genta, T. Iwaya, M. Sasaki, M. Goto and T. Hirose, *Ind. Eng. Chem. Res.*, 2005, 44, 3894−3900. https://doi: 10.1021/ie0488187
5. R. K. Soni and S. Singh, *J. Appl. Polym. Sci*., 2005, 96, 1515-1528. https://doi.org/10.1002/app.21502
6. R. Shamsi, M. Abdouss, G. M. M. Sadeghi and F. A. Taromi, *Polym. Int*., 2009, 58, 22-30. https://doi.org/10.1002/pi.2488
7. N. Tarannum, R. Agrawal and R. K. Soni, *Der. Pharma. Chemica.*, 2016, 8, 137-145.
8. J. Aguado and D. Serran, Feedstock Recycling of Plastic Wastes, Royal Society of Chemistry, London UK, 1999.
9. A. Jain and R. K. Soni, *J. Polym. Res.*, 2007, 14, 475-481. https://doi.org/10.1007/s10965-007-9131-9
10. A. S. Goje and S. Mishra, *Macromol. Mater. Eng.*, 2003, 288, 326-336. https://doi.org/10.1002/mame.200390034
11. D. E. Nikles and M. S. Farahat, *Macromol. Mater. Eng.*, 2005, 290, 13-30. https://doi.org/10.1002/mame.200400186
12. S. R. Shukla and A. M. Harad, *J. Appl. Polym. Sci*., 2005, 97, 513-517. https://doi.org/10.1002/app.21769

View Article Online
DOI: 10.1039/C9NJ01560D

13. G. P. Karayannidis and D. S. Achilias, *Macromol. Mater. Eng.*, 2007, 292, 128-146. https://doi.org/10.1002/mame.200600341
14. M. Y. Abdelaal, T. R. Sobahi and M. S. I. Makki, *Constr. Build. Mater.*, 2011, 25, 3267-3271. https://doi.org/10.1016/j.conbuildmat.2011.03.013
15. C. G. Namboori and M. S. Haith, *J. Appl. Polym. Sci.*, 1968, 12, 1999-2005. https://doi.org/10.1002/app.1968.070120901
16. D. Paszun and T. Spychaj, *Ind. Eng. Chem. Res.*, 1997, 36, 1373 -1383. https://doi.org/10.1021/ie960563c
17. S. Mishra, A. S. Goje and Zope, *Polym. React. Eng.*, 2003, 11, 79-99. https://doi.org/10.1081/PRE-120018586
18. S. Mishra, V. S. Zope and A. S. Goje, *J. Appl. Polym. Sci.*, 2003, 90, 3305-3309. https://doi.org/10.1002/app.13065
19. V. K. Sinha, M. R. Patel and J. V. Patel, *J. Polym. Environ.*, 2010, 18, 8-25. https://doi.org/10.1007/s10924-008-0106-7
20. R. Agrawal, N. Tarannum, M. Chourasia and R. K. Soni, *J. Polym. Environ.*, 2018, 26, 819-829. https://doi.org/10.1007/s10924-017-0987-4
21. Y. S. Parab and S. R. Shukla, *Waste. Biomass. Valor.*, 2013, 4, 23-27. https://doi.org/10.1007/s12649-012-9128-4
22. S. R. Shukla and A. M. Harad, *Polym. Degrad. Stab.*, 2006, 91**,** 1850-1854. https://doi.org/10.1007/s10924-008-0106-7
23. A. S. Goje, S. A. Thakur, V. R. Diware, Y. P. Chauhan and S. Mishra, Polym. *Plast. Technol. Eng.*, 2004, 43, 407-426. https://doi.org/10.1081/PPT-120029971
24. D. S. Achilias, G. P. Tsintzou, A. K. Nikolaidis, D. N. Bikiaris and G. P. Karayannidis*Polym. Int.*, 2011, 60, 500-506. https://doi.org/10.1002/pi.2976
25. V. S. Palekar, R. V. Shah and S. R. Shukla, *J. Appl. Polym. Sci.*, 2012, 126**,** 1174-1181. https://doi.org/10.1002/app.36878
26. Y. S. Parab, R. V. Shah and S. R. Shukla, *Curr. Chem. Lett.*, 2012, 1**,** 81-90.

View Article Online
DOI: 10.1039/C9NJ01560D

http://dx.doi.org/10.5267/j.ccl.2012.3.003

27. G. M. M. Sadeghi, R. Shamsi and M. Sayaf, *J. Polym. Environ.*, 2011, 19, 522-534. https://doi.org/10.1007/s10924-011-0283-7
28. V. S.Palekar, A. J.Damle and S. R. Shukla, *Eur. J. Med. Chem.*, 2009, 44, 5112-5116. https://doi.org/10.1016/j.ejmech.2009.07.023
29. R. K. Soni, K. Dutt, A. Jain, S. Soam and S. A. Singh, *J. Appl. Polym. Sci.*, 2009, 113, 1090-1096. https://doi.org/10.1002/app.29842
30. R. Agrawal, N. Tarannum, S. Mishra and R. K. Soni, *Der. Pharma. Chemica.*, 2016, 8, 132-139. http://derpharmachemica.com/archive.html
31. R. K. Soni, M. Teotia and K. Dutt, *J. Appl. Polym. Sci.*, 2010, 118, 638-645. https://doi.org/10.1002/app.32377
32. M. Teotia and R. K. Soni, J. Ind. Chem. Soc., 2016, 93, 639-648.
33. M. Teotia and R. K. Soni, *J. Sci. Ind. Res.*, 2017, 6, 160-165. http://nopr.niscair.res.in/handle/123456789/40648
34. M. Teotia and R. K. Soni, *Eng. Fail. Anal.*, 2018, 94, 412-437. https://doi.org/10.1016/j.engfailanal.2018.08.016
35. J. Macan, I. Brnardić, M. Ivanković and H. J. Mencer, *J. Therm. Anal. Calorim.*, 2005, 81, 369-373. https://doi.org/10.1007/s10973-005-0794-3
36. R. Seifi and M. Hojjati, *J. Comp. Mater.*, 2005, 39, 1027-1039. https://doi.org/10.1177%2F0021998305048738
37. M. Teotia, M. Chauhan, P. Choudhary, and R. K. Soni, *J. Therm. Anal. Calorim.*, 2018, 113, 1-9. https://doi.org/10.1007/s10973-018-7907-2
38. T. Maity, B. C. Samanta, S. Dalai, and A. K. Banthia, *Mater. Sci. Eng. A.*, 2007, 464, 38-46. https://doi.org/10.1016/j.msea.2007.01.128
39. A. M. Atta, R. Mansour and M. I. Abdou, *Polym. Adv. Technol.*, 2004, 15, 514-522. https://doi.org/10.1002/pat.507

View Article Online
DOI: 10.1039/C9NJ01560D

40. A. M. Atta, R. Mansour, M. I. Abdou and A. M. El-Sayed, *J. Polym. Res.*, 2005, 12, 127-138. https://doi.org/10.1007/s10965-004-2936-x
41. G. R. Saad and A. F. S. Eldin, *J. Therm. Anal. Calorim.*, 2012, 110, 1425-1430. https://doi.org/10.1007/s10973-011-2074-8
42. N. Rabearison, C. Jochum and J. C. Grandidier, *J. Mater. Sci.*, 2011, 46, 787-796. https://doi.org/10.1007/s10853-010-4815-7
43. M. Teotia, N. Tarannum and R. K. Soni, *J. Appl. Polym. Sci.*, 2017, 134, 45153. https://doi.org/10.1002/app.45153
44. A. X. S. Bruker and W. I. Madison, SAINT+ Software for CCD Diffractometers, 2000.
45. G. M. Sheldrick, SADABS 2.0, 2000.
46. L. Krause, I. R. Herbst, G. M. Sheldrick and D. Stalke, *J. Appl. Crystallogr.*, 2015, 48, 3-10. https://doi.org/10.1107/S1600576714022985
47. K. Bradenburg, Diamond, version 3.1e, Crystal Impact GbR, Bonn (Germany), 2005.
48. M. Frisch, G. W. Trucks, H. B. Schlegel, G. E. Scuseria, M. A. Robb, J. R. Cheeseman, J. A. Montgomery Jr, T. Vreven, K. N. Kudin, J. C. Burant and J. M. Millam, Gaussian 03, revision D. 01. Gaussian Inc., Wallingford, CT 26, 2004.
49. P. Hohenberg and W. Kohn, *Phys. Rev.*, 1964, 136, 864-871.
50. W. Kohn and L. Sham, Phys Rev., 1965, 140, 1133-1138. https://doi.org/10.1103/PhysRev.140.A1133
51. A. D. Becke, *J. Chem. Phys.*, 1993, 98, 5648-5652.
52. H. Chmara, R. Andruszkiewicz and E. Borowski, *Biochem. Biophys. Res. Commun.*, 1984, 120, 865-872. https://doi.org/10.1016/S0006-291X(84)80187-4
53. N. J. Marshall, R. Andruszkiewicz, S. Gupta, S. Milewski and J.W. Payne *J. Antimicrob. Chemother*., 2003, 51, 821–831 https://doi.org/10.1093/jac/dkg170
54. S. Milewski, H. Chmara, R. Andruszkiewicz, E. Borowski, M. Zaremba and J. Borowski *Drugs. Exp. Clin. Res.*, 1988, 14, 461-465.
55. H. V. Bossche and L. Koymans, *Mycoses.*, 1998, 41, 32-38.
56. D. J. Sheehan, C. A. Hitchcock and C. M. Sibley, *Clin. Microbiol. Rev.*, 1999, 12, 40-79.

View Article Online
DOI: 10.1039/C9NJ01560D

https://doi.org/10.1128/CMR.12.1.40

57. Y. Yoshida, Y. Aoyama, M. Noshiro and O. Gotoh, *Biochem. Biophys. Res. Commun.*, 2000, 273, 799-804. https://doi.org/10.1006/bbrc.2000.3030
58. G. M. Morris, R. Huey, W. Lindstrom, M. F. Sanner, R. K. Belew, D. S. Goodsell and A. J. Olson, *J. Comput. Chem.*, 2009, 16, 2785-2791. https://doi.org/10.1002/jcc.21256
59. W. L. DeLano, PyMOL. DeLano Scientific, (San Carlos) CA, 700, 2002.
60. G.O. Spessard, *J. Chem. Inf. Comput. Sci.*, 1998, 38 (6), 1250–1253 https://doi.org/10.1021/ci980264t
61. D. M. F. van Aalten, R. Bywater, J. B. C. Findlay, M. Hendlich, R. W. W. Hooft, and G. Vriend, *J. Comput.-Aided Mol. Des.*, 1996, 10, 255-262. https://doi.org/10.1007/BF00355047
62. H. E. Gottlieb, V. Kotlyar and A. Nudelman, *J. Org. Chem.*, 1997, 62, 7512-7515.
63. G. R. Fulmer, A. J. Miller, N. H. Sherden, H. E. Gottlieb, A. Nudelman, B. M. Stoltz, J. E. Bercaw and K.I Goldberg, *Organometallics*, 2010, *29*(9), 2176-2179. https://doi.org/10.1021/om100106e
64. Y. C. Ning and R. R. Ernst, Structural identification of organic compounds with spectroscopic techniques. Weinhem:Willey-VCH, 2005.
65. A. Lather, S. Sharma and A. Khatkar, *Comb. Chem. High Throughput Screen*, 2018, 21(3), 182-193. https://doi.org/10.2174/1386207321666180330114457

View Article Online
DOI: 10.1039/C9NJ01560D

Molecular structures of two isomers have been investigated by SXRD analysis and DFT calculations and the isomers are assessed for antimicrobial properties and curing agents for epoxy resins.